STEM CELLS®

TECHNOLOGY DEVELOPMENT

Fluorophore-Conjugated Iron Oxide Nanoparticle Labeling and Analysis of Engrafting Human Hematopoietic Stem Cells

DUSTIN J. MAXWELL,[a] JESPER BONDE,[b] DAVID A. HESS,[c] SARAH A. HOHM,[b] RYAN LAHEY,[d] PING ZHOU,[d] MICHAEL H. CREER,[e] DAVID PIWNICA-WORMS,[a] JAN A. NOLTA[d]

[a]Molecular Imaging Center, Mallinckrodt Institute of Radiology, Department of Molecular Biology and Pharmacology, [b]Division of Oncology, Hematopoietic Development and Malignancy Program, Washington University School of Medicine, St. Louis, Missouri, USA; [c]Vascular Biology Program, Robarts Research Institute, London, Ontario, Canada; [d]Department of Internal Medicine, Stem Cell Program, University of California-Davis, Sacramento, California, USA; [e]Departments of Pathology and Laboratory Medicine, Saint Louis University School of Medicine, St. Louis, Missouri, USA

Key Words. Feridex • Iron oxide • Nanoparticle • Immune-deficient mice • Human stem cells • Hematopoiesis • Transplantation

ABSTRACT

The use of nanometer-sized iron oxide particles combined with molecular imaging techniques enables dynamic studies of homing and trafficking of human hematopoietic stem cells (HSC). Identifying clinically applicable strategies for loading nanoparticles into primitive HSC requires strictly defined culture conditions to maintain viability without inducing terminal differentiation. In the current study, fluorescent molecules were covalently linked to dextran-coated iron oxide nanoparticles (Feridex) to characterize human HSC labeling to monitor the engraftment process. Conjugating fluorophores to the dextran coat for fluorescence-activated cell sorting purification eliminated spurious signals from nonsequestered nanoparticle contaminants. A short-term defined incubation strategy was developed that allowed efficient labeling of both quiescent and cycling HSC, with no discernable toxicity in vitro or in vivo. Transplantation of purified primary human cord blood lineage-depleted and CD34$^+$ cells into immunodeficient mice allowed detection of labeled human HSC in the recipient bones. Flow cytometry was used to precisely quantitate the cell populations that had sequestered the nanoparticles and to follow their fate post-transplantation. Flow cytometry endpoint analysis confirmed the presence of nanoparticle-labeled human stem cells in the marrow. The use of fluorophore-labeled iron oxide nanoparticles for fluorescence imaging in combination with flow cytometry allows evaluation of labeling efficiencies and homing capabilities of defined human HSC subsets. STEM CELLS *2008;26:517–524*

Disclosure of potential conflicts of interest is found at the end of this article.

INTRODUCTION

Highly purified human hematopoietic stem cells (HSC) are identified functionally by performing in vivo repopulation studies in immune-deficient animals. Previous in vivo studies of human HSC homing and engraftment have been performed using genetic labels, radionuclides, or membrane dyes [1]. Although efficient, these techniques encompass a number of limitations. Genetic modification of cells with a reporter gene carries a low but real risk of permanently altering the phenotype or behavior of the target cell [2]. High doses of radionuclides or membrane dyes can also be toxic to cells. Researchers are therefore examining alternative methods to label HSC and track their migration in vivo, which were the goals of the current study.

Recently, long-term repopulating cells labeled with native or dextran-coated superparamagnetic iron oxide nanoparticles (SPIOs) have been tracked using magnetic resonance imaging (MRI) [3–8]. SPIOs such as Feridex are inert, biocompatible nanoparticles that are eventually metabolized and enter into whole body iron metabolism pathways. Feridex (Bayer Healthcare, Cambridge, MA, http://imaging.bayerhealthcare.com/html/feridex/index.html) is approved as a contrast agent for imaging of the liver after i.v. infusion of the contrast agent, but it is not currently U.S. Food and Drug Administration (FDA)-approved for cell labeling or cell tracking. Because dextran-coated SPIOs have an inherent negative surface charge, they inefficiently label human stem cells and other mammalian cell types, with the exception of phagocytic cells, such as macrophages. To overcome this limitation, a number of approaches have been described to modify the dextran coating to facilitate uptake in specific cell populations. The primary labeling approach involves complexing polycationic transfection agents with SPIOs [9–13]. Other examples include conjugating Tat peptides or cell-specific antibodies to the dextran coat to increase labeling efficiencies [7, 14–17].

Electrostatic interactions between polycationic materials and the dextran coat form stable complexes that can bind to the cell membrane and enter the cell through pinocytosis and/or endocytosis-mediated pathways. Of the polycationic transfection agents, protamine sulfate is particularly suited for in vivo studies because it is FDA-approved, currently used in clinical trials examining gene transduction by retroviral vectors, and

Correspondence: Jan A. Nolta, Ph.D., Stem Cell Program, University of California at Davis, Room 653, 2425 Stockton Boulevard, Sacramento, California 95817, USA. Telephone: 916-453-2335; Fax: 916-453-2173; e-mail: Jan.nolta@ucdmc.ucdavis.edu Received January 15, 2007; accepted for publication November 9, 2007; first published online in STEM CELLS *EXPRESS* November 29, 2007; available online without subscription through the open access option. 1066-5099/2008/$30.00/0 doi: 10.1634/stemcells.2007-0016

exhibits a lower toxicity toward cells compared with other polycationic species [11]. Defining ex vivo cultivation strategies for the labeling of HSC populations with nanoparticles must involve the use of strictly defined in vitro culture conditions with the aim of maintaining target cell viability without inducing terminal differentiation or damaging the homing and engraftment potential of the target cells.

In the current study, two agents, Feridex and protamine sulfate, were used to label human HSC populations under defined, clinically applicable, serum-free ex vivo conditions for subsequent tracking. To assess the labeling efficiencies in cells with different phenotypes, as assessed by flow cytometry, red-shifted Alexa Fluor dye molecules were covalently linked to the dextran coat of Feridex (Fe[647] or Fe[750]). Compared with the traditional analysis of Feridex labeling by staining cells with Prussian Blue or anti-dextran fluorophores, signals generated from the Fe[647]- and Fe[750]-labeled human HSC subsets in the current studies could be analyzed by flow cytometry to precisely quantitate the cell populations that had sequestered the nanoparticles and to follow their fate post-transplantation. Importantly, conjugating fluorophores to the dextran coat allowed nanoparticle-labeled $CD34^+$ cells to be fluorescence-activated cell sorting (FACS)-purified, thus eliminating the resulting signal in vivo from nonsequestered nanoparticle contaminants. Endpoint analysis of purified $Fe[750]^+CD34^+$ cells transplanted into immunodeficient NOD/SCID β2M-null mice showed that labeled cells could be detected for up to 3 weeks. Fluorescence imaging and flow cytometry analysis of both the bone marrow and hematopoietic organs revealed the presence of $Fe[750]^+CD34^+$ cells.

The current study provides a method by which investigators can track human stem cells to the marrow versus different tissues of immune-deficient mice. This has been extremely difficult in the past, because stem cells can alter their phenotype after engraftment. The fluorophore-tagged Feridex allows a clean recovery of labeled cells from different tissues by FACS for cell surface phenotype probing and other assays. Traditional staining methods with Prussian blue and antidextran fluorophores can show that cells are Feridex-positive but do not permit a quantitative determination of engraftment post-transplantation. Because of the fluorophore modification, quantitation of the number of cells that are engrafted in the bone marrow after transplantation is possible and allows simultaneous probing of cell surface phenotype using flow cytometry, without the requirement for isolating cells based on a predetermined cell surface marker. The use of fluorophore-labeled Feridex nanoparticles and the clinically relevant incubation procedure described in the current study offer an efficient and safe method to label both cycling and noncycling human hematopoietic stem and progenitor cells without toxicity and to evaluate the homing, localization, phenotype, and short-term engraftment capabilities of defined human HSC subsets.

Materials and Methods

Cell Sources

Human umbilical cord blood (CB) samples were obtained from the cord blood banking facility at Cardinal Glennon Children's Hospital (St. Louis, MO). Human bone marrow (BM) samples were obtained from the Oncology Division at the Siteman Cancer Center (St. Louis, MO). Use of these samples was approved by the local ethical and biohazard authorities at Washington University School of Medicine (St. Louis, MO). Mononuclear cells (MNC) were isolated by gradient density centrifugation using Ficoll-Hypaque (Amersham Pharmacia Biotech Inc., Uppsala, Sweden, http://www.biobank.co.kr/maker/aaa/amersham.shtml). MNC from CB and BM were enriched for CD34 antigen-positive cells using a Miltenyi AutoMACS device in accordance with the specifications from the manufacturer (Miltenyi Biotec, Auburn, CA, http://www.miltenyibiotec.com). The purity of the $CD34^+$ cells was determined using single-parameter analysis on an FC500 flow cytometer (Beckman Coulter, Hialeah, FL, http://www.beckmancoulter.com) after labeling with a directly anti-human allophycocyanin (APC)-conjugated monoclonal antibody (MoAb) (CD34 class III-APC; Dako, Glostrup, Denmark, http://www.dako.com). The $CD34^+$ purity was in all cases >90%. Lin^- preparations were isolated as previously described [18].

Preparation of Fe[647] and Fe[750] Nanoparticles

Synthesis of Alexa Fluor 647- and Alexa Fluor 750-conjugated Feridex (Fe[647] and Fe[750], respectively) was based on previously published methods [15]. Briefly, 1 ml of Feridex (11.2 mg/ml) was added to a solution containing 1.6 ml of KOH, 0.7 ml of double-distilled H_2O (ddH_2O), and 0.7 ml of epichlorohydrin [19]. The mixture was reacted for 12 hours with constant shaking. To produce reactive amines on the dextran coat, concentrated ammonia (0.5 ml) was added to the Feridex and reacted overnight at 37°C. Excess epichlorohydrin and ammonia were removed by extensive dialysis against ddH_2O using 12,000–14,000 molecular weight cut off tubing. Feridex was reacted with 1 mg of Alexa Fluor 647 or 750 succinimidyl ester (Molecular Probes, Eugene, OR, http://probes.invitrogen.com) overnight at room temperature. Excess fluorophore was removed by centrifuging the sample at 160,000*g* for 30 minutes. The supernatant was discarded, and the pellet was resuspended in phosphate-buffered saline (PBS) buffer (pH 7.4). The centrifugation step was repeated four times to ensure that unconjugated fluorophore was removed from the sample. Removal of excess fluorophore was confirmed using a fluorometer. To disperse and remove large nanoparticle aggregates, the sample was sonicated for 5 minutes and filtered using a 0.2 μM size-exclusion filter.

The iron concentration was measured using the method described by Stookey [20]. The number of fluorescent molecules was calculated by using a standard curve of known Alexa Fluor 750 concentration. From these measurements, assuming an average particle diameter of 80 nm, we determined that there were approximately 140 molecules per iron particle.

Labeling Protocol

Cell cultivation was carried out in 96-well tissue culture-treated plates coated with the recombinant fibronectin fragment CH-296 (25 $\mu g/cm^2$) (RetroNectin; TaKaRa Shuzo, Kyoto, Japan, http://www.transnationale.org/companies/takara_shuzo.php) as described [21–23]. X-Vivo 15 defined serum-free medium (BioWhittaker Inc., Walkersville, MD, http://www.devicelink.com/company/ivdt/b/b0092.html) was supplemented with 10 ng/ml thrombopoietin, recombinant human stem cell factor (rhSCF), and Flt-3-ligand (R&D Systems Inc., Minneapolis, http://www.rndsystems.com). Cells were plated at 2×10^5 cells per well in 200 μl of medium. A stock solution of 100 μg/ml Fe[647] or Fe[750] was prepared in medium, and protamine sulfate (Pro) (American Pharmaceuticals, Schaumberg, IL, http://www.appdrugs.com/) was added 20 minutes prior to use at a final concentration of 10 μg/ml. The Pro-Fe[647] complex was added to the cells at a final concentration of 12.5 μg/ml and incubated overnight at 37°C, 5% CO_2, and ambient oxygen (21%). No differences in loading efficiencies were observed between cultures incubated with Pro-Fe[647] and those incubated with Pro-Fe[750]. Cultured cells were harvested at specific time points using enzyme-free PBS-based cell dissociation buffer (Gibco, Grand Island, NY, http://www.invitrogen.com) to release cells from integrin-mediated adhesion to the CH-296-coated plates.

Clonogenic Progenitor Assay

Human clonogenic progenitor assays were performed by plating 1,000 cells from the ex vivo cultures into methylcellulose medium (Methocult H4434; StemCell Technologies, Vancouver, BC, Canada, http://www.stemcell.com) containing 50 ng/ml rhSCF, 10 ng/ml recombinant human granulocyte colony-stimulating factor,

Table 1. Nanoparticle labeling of mononuclear cells vs. enriched stem/progenitor cell fractions

Cell type	*n*	Nano$^+$ total	CD34$^+$ total	CD133$^+$ total	CD34$^+$/nano$^+$	CD133$^+$/nano$^+$
MNC	3	28.1% ± 3%	7% ± 1.4%	4.4% ± 4.5%	6.2% ± 0.8%	3.5% ± 5%
Lin$^-$	7	39% ± 23.7%	34.7% ± 11.5%	27.7% ± 17%	8.8% ± 3.3%	5.7% ± 2.6%
CD34$^+$	6	37.6% ± 15.8%	90% ± 3.6%	79.4% ± 20.1%	31.8% ± 13.9%	26.7% ± 18.3%

Umbilical cord blood-derived MNC, Lin$^-$, and CD34$^+$ purified cells were incubated overnight with Pro-Fe[647] particles. The hematopoietic stem/progenitor cell surface markers CD34 and CD133 were assessed by fluorescence-activated cell sorting analysis to determine the percentage of Fe[647] nanoparticle uptake in each progenitor cell population.
Abbreviations: Lin$^-$, lineage-negative; MNC, mononuclear fraction; Nano$^+$, CD45$^+$ cells that colabeled for nanoparticle content.

and 10 ng/ml recombinant human interleukin 3. Cells (1,000 cells per ml of medium per dish) were plated in gridded colony-forming unit (CFU) dishes. Colony-forming capacity was evaluated as described [24] by enumeration under light microscopy following 14 days incubation at 37°C, 5% CO_2.

Transplantation

NOD/SCID microglobulin (B2M)-null mice [25, 26] were obtained from the Jackson Laboratory (Bar Harbor, ME, http://www.jax.org). The studies were approved by the Animal Studies Committee at Washington University. Six- to 8-week-old mice were irradiated with 300–350 cGy prior to transplantation. Mice were then transplanted by i.v. or intrafemoral (i.f.) routes with 5×10^5 FACS-sorted Fe[750]$^+$CD34$^+$ cells. A series of control mice received 5×10^5 unlabeled CD34$^+$cells, free Fe[750] particles, PBS buffer, or unsorted bulk cultures consisting of a mixed population of Fe[750] particles and labeled Fe[750]$^+$CD34$^+$ cells. Animals were sacrificed at defined time points between 24 hours and 8 weeks post-transplantation. Bones and spleen were collected from each mouse as described [27, 28] for subsequent analyses by flow cytometry and fluorescence imaging.

Flow Cytometry Analysis

Harvested cells were resuspended in PBS, and cellular Fc receptors were blocked by addition of purified rat anti-mouse CD16/CD32 (fc_δIII/II receptor) MoAb (BD Pharmingen, San Diego, http://www.bdbiosciences.com/index_us.shtml). Forward and orthogonal light scattering were used to exclude debris and dead cells. For the extended analysis of the iron label in defined HSC subsets, as well as to assess engraftment in transplanted NOD/SCID β2M-null mice, multiparameter flow cytometry using directly conjugated human-specific CD34 and CD45 MoAbs (DakoCytomation, Glostrup, Denmark, http://www.dakocytomation.com) was performed. The human CD133/2-PE MoAb was obtained from Miltenyi Biotec. Cells were analyzed on a Coulter FC500 flow cytometer (Beckman Coulter) using the software provided. FACS was performed using a custom-modified MoFlo sorter (DakoCytomation).

Fluorescence Imaging

Imaging was performed using a Kodak 4000MM multimodal imager (Kodak, Rochester, NY, http://www.kodak.com) equipped with an IS4000MM charge-coupled device camera. The instrument settings were as follows: focal plane, 13 mm; zoom, 60 mm; f-stop, open; x-ray acquisition time, 20 seconds; fluorescence acquisition time, 60 seconds; excitation filter, 750 wavelength (WA); emission filter, 800 WA; binning, 2 × 2. Animals were imaged pre- and postinjection, at 24 hours, and at 1-week intervals up to 3 weeks. An x-ray image was acquired for 20 seconds prior to fluorescence image. The fluorescent images were acquired for each cohort of animals using the setting described in Materials and Methods. Fluorescent images were overlaid on the corresponding x-ray images (i.e., a fused image). Data analysis was performed using the Kodak software. Each image was background subtracted using background x-ray and fluorescence images. Fluorescent images were evaluated using the intensity scale (included in Fig. 5) and quantitatively assessed to determine mean fluorescence intensity by drawing a region of interest around each bone sample.

Prussian Blue Staining

Frozen muscle sections were fixed in 10% neutral buffered formalin (Sigma-Aldrich, St. Louis, http://www.sigmaaldrich.com) followed by washing in H_2O. Tissues were incubated for 30 minutes with 5% potassium ferrocyanide in 6% hydrochloric acid, washed, and counterstained with nuclear fast red. Images were taken using a Zeiss microscope (Carl Zeiss, Jena, Germany, http://www.zeiss.com).

Statistical Analyses

Data were expressed as mean values based upon a number of observations ± SD. Statistical analysis was performed using a two-tailed Student's *t* test with equal variance. Values were considered significantly different at the 95% confidence level.

Results

Labeling Human Stem/Progenitor Cell Subsets

To optimize the loading protocol, we examined different HSC subsets derived from human umbilical CB. Mononuclear fractions (MNC fraction), lineage-depleted cells (Lin$^-$), and CD34$^+$ populations were incubated overnight with complexed protamine sulfate Alexa Fluor 647-conjugated Feridex (Pro-Fe[647]). We used plates coated with the fibronectin fragment retronectin in all ex vivo culture protocols to sustain human stem cell viability and maintenance of primitive reconstituting capacity, as we have previously published [21, 24]. Analysis of each subset was performed by correlating the signal from Fe[647]-labeled cells to the human HSC markers CD34 and CD133. Flow cytometric measurements of the total MNC population showed an average of 28.1% ± 3.0% Fe[647]-labeled cells (Table 1). Correlating the Fe[647] signal to CD34$^+$ and CD133$^+$ showed that the majority of Fe[647]-positive (Fe[647]$^+$) cells within the bulk MNC population were differentiated cells, rather than stem or progenitor cells (Table 1). Subsequent delineation of the Fe[647]$^+$ cells showed that these were of monocytic (CD14) or myeloid (CD13) lineages (data not shown), which agrees with recently published data [29–32]. Removal of mature cells by negative selection and labeling the Lin$^-$ fraction showed that an average of 39% ± 23.7% of the total cells were Fe[647]$^+$. Further analysis of these Fe[647]-labeled cells revealed that 8.8% ± 3.3% and 5.7% ± 2.6% were CD34$^+$ and CD133$^+$, respectively.

Positive selection of CD34$^+$ cells from the MNC prior to labeling with Pro-Fe[647] resulted in an increase in nanoparticle labeling (Fig. 1; Table 1). These data indicate that labeling efficiencies are dependent on the degree of purification of target cells. CD34 selection resulted in a cell population with more than 95% purity for labeling. Loading profiles of CD34$^+$ cells from cord blood were compared with those of CD34$^+$ cells enriched from human BM. Human BM CD34$^+$ cells consistently attained levels of Fe[647] labeling similar to those of CB CD34$^+$ cells (31.8% ± 13.9% Fe[647]$^+$CD34$^+$ in CB and 24.4% ± 11.4% Fe[647]$^+$CD34$^+$ in BM). Increasing the Pro-

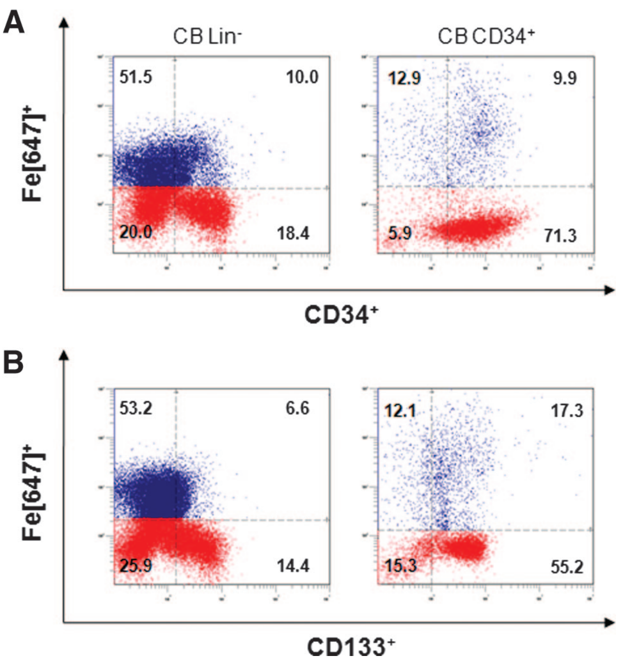

Figure 1. Representative flow cytometry analysis of Fe[647]-labeled Lin^- and $CD34^+$ cells. Human cells derived from CB were sorted by positive selection for CD34 ($CD34^+$) or by negative selection using lin^-, labeled with Fe[647] nanoparticles, and analyzed for expression of CD34 ($n = 7$) **(A)** or CD133 ($n = 6$) **(B)** after overnight incubation. Abbreviations: CB, cord blood; Lin, lineage.

Fe[647] concentration or incubation period had little effect on the overall loading efficiency. FACS side scattering plots of these samples showed large excesses of free Fe[647] particles in culture, whereas much higher particle concentrations resulted in cell distortion and, in extreme cases, cell death (data not shown).

Cell Cycle, Viability, and Clonogenic Potential

To allow accurate tracking of human progenitors to the marrow and other tissue compartments in vivo, it is important to determine whether both cycling and noncycling human stem and progenitor cells sequester nanoparticles in an equivalent manner. Retroviral vectors, also used for cell marking and tracking, will only transduce cells that pass through mitosis [33], and lentiviral vectors require metabolic activation to progress from the G0 to the G1 phase of the cell cycle prior to viral integration [34]. A method is thus needed that allows marking of quiescent cells. To evaluate nanoparticle labeling as a function of cell cycle status, $CD34^+$ cells from CB were labeled with a membrane dye (PKH26) to characterize cell proliferation over a 72-hour period. Labeled $Fe[750]^+CD34^+$ cells were harvested at 24-hour intervals and analyzed by flow cytometry. Gating on the emission of PKH26 shows that after 72 hours of culture, 25.8% of the cells had divided twice, 56.3% had divided once, and the remaining 16.9% of the cells had not divided (Fig. 2). Each cell population, gated based on division history, was examined to assess the percentage of $Fe[750]^+CD34^+$ cells. Of the cells that had actively divided, 16.7% of the total cell population that had divided once and 12% of the cells that had divided twice were $Fe[750]^+CD34^+$. Within the cell population that had not proliferated, 26.4% of cells were $Fe[750]^+CD34^+$. These data demonstrate that quiescent cells can be labeled at least as efficiently as dividing cells using Fe[750]. These data emphasize an advantage for the use of nanoparticles over the use of viral transduction for short-term in vivo tracking studies, that is, the potential labeling of quiescent cells and also avoiding the risk of adverse effects that viral transduction and potential insertional integration could potentially impose on human HSC [35].

Clonogenic progenitor assays were performed as an initial test to evaluate whether there were potential negative effects of the nanoparticle labeling on cell survival and proliferation. CB Lin^- cells were incubated overnight with and without Pro-Fe[647]. Harvest cells were plated into semisolid methylcellulose medium for assessment of clonogenic potential. The colony-forming capacities from nanoparticle-labeled and nonlabeled cells derived from the same source are summarized in Table 2. The CFU potential did not significantly differ between human Lin^- cells subjected to Pro-Fe[647] and the cells that had been cultured in identical conditions but with no nanoparticles. These data demonstrate that labeling cells with Fe[647] does not affect the overall clonogenic capacity of purified hematopoietic progenitor cells. The regenerative capacity of more primitive, Fe[647]-labeled stem cells was then assessed using an in vivo murine xenotransplantation model.

Tracking Labeled Cells in NOD/SCID β2M-Null Mice

We investigated the time period after transplantation in which the labeled cells could be tracked, and we determined whether the labeling strategy imposed any adverse effects on human stem cell homing or on the subsequent hematopoietic contribution in vivo. $CD34^+$ cells were cultured overnight with Fe[647] particles, and the labeled cell population contained a total of 24% $Fe[647]^+$ human $CD34^+$ cells. Labeled cells were acquired using flow cytometer-based cell sorting to remove unlabeled cells and free Fe[647] contaminants. NOD/SCID β2M-null mice ($n = 15$) were then transplanted with Fe[647]-labeled human CB-derived $CD34^+$ cells. Mice transplanted with the sorted cells were sacrificed at 1, 2, and 3 weeks. The femurs and tibiae from each animal were flushed with PBS buffer, and the collected marrow cells were assessed for the percentages of Fe[647]-labeled and unlabeled human CD45-positive cells. Endpoint analyses at weeks 1 ($n = 4$) and 2 ($n = 6$) showed similar engraftment between total $CD45^+$ cells and $CD45^+$ cells that colabeled for nanoparticle content (Fig. 3A). The data suggested continued accrual of labeled cells to the marrow compartment over the first 2 weeks. Cell migration from sites of nonspecific lodgment into the bone marrow over the initial 2 weeks post-transplantation has previously been reported [36]. At week 3, engraftment constituted 9.5% ± 6.2% $CD45^+$ cells in the chimeric BM ($n = 5$), with only 0.6% ± 0.4% $Fe[647]^+$. By this point, the human cells had expanded sufficiently to dilute out the nanoparticle label, or the particles had been at least partially degraded [37], but label was still observed in a small number of the human $CD45^+$ cells. These data demonstrate that there was no loss in long-term viability, marrow homing, or hematopoietic capacity of human hematopoietic stem cells caused by the labeling procedure and that the cells retained label sufficient for analysis for the initial 2 weeks post-transplantation.

Prussian blue staining was done on muscle tissue from several of the engrafted mice to visually locate hematopoietic cells that may have lodged in nonhematopoietic sites, as a first step in tracking labeled cells following bone marrow engraftment. Figure 3B shows Prussian blue staining of Feridex-labeled cells in the muscle tissue adjacent to the femur of a mouse transplanted with 5×10^5 labeled human $CD34^+$ progenitors.

To increase the sensitivity of in situ detection, we used red-shifted Fe[750] nanoparticles in subsequent assays. Figure 4 is a representative example from the transplantation experiments using Fe[750] nanoparticle-loaded cells. Figure 4A shows the forward and side scatter plot, which demonstrates the impor-

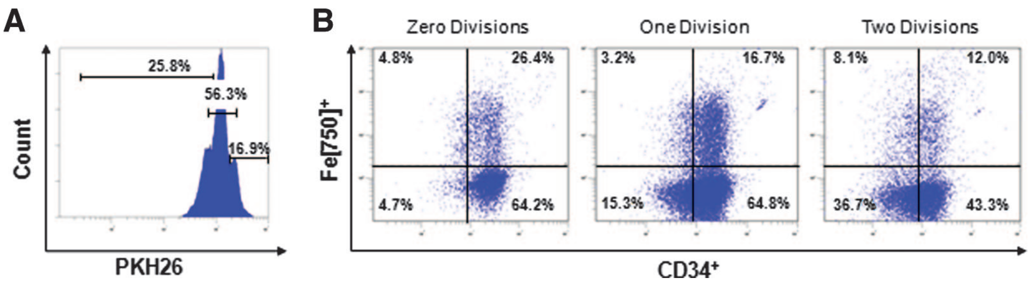

Figure 2. Cell proliferation assay of labeled CD34$^+$ cells. Cultured Fe[750]$^+$CD34$^+$ cells were labeled with the membrane dye PKH26. **(A):** Flow cytometry analysis gating on the emission of PKH26 shows the number of cell divisions at 72 hours. **(B–D):** Individual histograms of cells having undergone zero (16.9%), one (56.3%), or two (25.8%) cell divisions were further analyzed by CD34 expression and Fe[750] signal to demonstrate that uptake in the undivided population was at least as high as in the fractions that had undergone division.

Table 2. Assessment of clonogenic potential in Fe[647] nanoparticle-labeled lineage$^-$ cells

Experimental setup	Colony delineation		
	CFU-GM	BFU-E	CFU-GEMM
+ Fe-Pro	51 ± 14.1	50.5 ± 12	0.5 ± 0.7
− Fe-Pro	55 ± 7.1	60 ± 0	3.5 ± 0.7
p value (+ vs. −)	>.05	>.05	>.05

Abbreviation: BFU-E, burst-forming unit-erythrocyte; CFU-GEMM, colony-forming unit granulocyte/erythrocyte/macrophage/megakaryocyte; CFU-GM, colony-forming unit granulocyte/macrophage; Pro, protamine sulfate.

tance of using flow sorting or another type of cell separation technique to remove unbound nanoparticles, which would have constituted 75% of unsorted counted events. The cells in the R1 gate, 25% of the total events, were isolated from the free nanoparticles using cell sorting, and the cells were further split into Fe[750]-low (R3 = 47.3%) and Fe[750]-high (R4 = 22.5%) populations for transplantation. Data from the transplantation of the nanoparticle-high cell fraction (R4) are shown below the sorting gates in Figure 4, obtained from the marrow of chimeric mice sacrificed at 2 and 4 weeks post-transplantation. The mouse analyzed at 2 weeks post-transplantation had a human cell engraftment of 4.3% in the BM, with 13.8% of these human cells in the chimeric marrow testing positive for Fe[750]. The mouse analyzed at 4 weeks postengraftment had a total human cell content of 29.2% in the marrow, but by that time point, the nanoparticle-labeled cells totaled only 2.8% of the human cells. By the 4-week time point, an increase in the human hematopoietic content of the chimeric mouse marrow and the very low amount of Fe[750] still contained in the human cells may indicate that the cells have divided multiple times in vivo, reducing the number of nanoparticles per cell.

In Situ Imaging of Labeled Cells in the Bone Marrow

To directly image the engraftment of the nanoparticle-labeled cells in the bone marrow of the recipient animals, Alexa Fluor 750 was conjugated to the dextran coat of Feridex. NOD/SCID β2M-null mice were transplanted i.v. and i.f. with 5 × 10^5 FACS-sorted CD34$^+$ Fe[750]$^+$ cells. The FACS-sorted cells were divided into two separate populations, Fe[750]^{hi}CD34$^+$ and Fe[750]^{lo}CD34$^+$ cells. A series of control mice was injected with PBS and free Fe[750] particles. Animals were sacrificed at 2 weeks, and the bones and the organs were removed from each animal and examined, in a side-by-side comparison, using fluorescence imaging.

Figure 5 shows bone and spleen images of a representative cohort of the transplanted NOD/SCID β2M-null mice after 2 weeks. The fluorescent signal emitted from the bone marrow indicates the presence of Fe[750]. An example of a mouse that had received a transplant of 4 × 10^5 Fe[750]^{lo}CD34$^+$ cells via i.v. injection is shown in Figure 5A. The signal from both right and left legs was low in this mouse. A mouse injected with the same cell sample but gated on the nanoparticle-high cells is shown in panel 5C. This mouse had received 4 × 10^5 Fe[750]^{hi}CD34$^+$ cells via i.v. injection. In comparison with the bones shown in Figure 5A, from the nanoparticle-low fraction, the signal in the bones was much stronger. The intensity of the spleen in this mouse was also high, indicating that a large

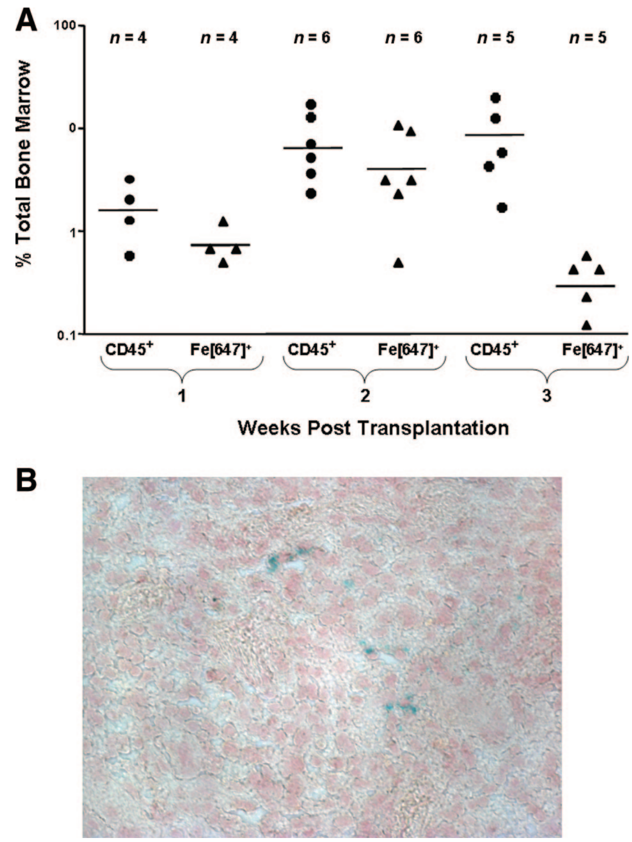

Figure 3. Summary of human engraftment in mice transplanted with Fe[647]$^+$CD34$^+$ resorted cultures. **(A):** Each mouse received a transplanted aliquot of fluorescence-activated cell sorting-purified cells via tail vein injection. Time points were generated by flow cytometry of flushed femurs and tibia from each animal at weeks 1 (n = 4), 2 (n = 6), and 3 (n = 5) by gating on the emission of human-specific CD45 and Fe[647]. **(B):** Prussian blue staining of Feridex-labeled cells in the muscle tissue adjacent to the femur of a mouse transplanted with 5 × 10^5 labeled human CD34$^+$ progenitors.

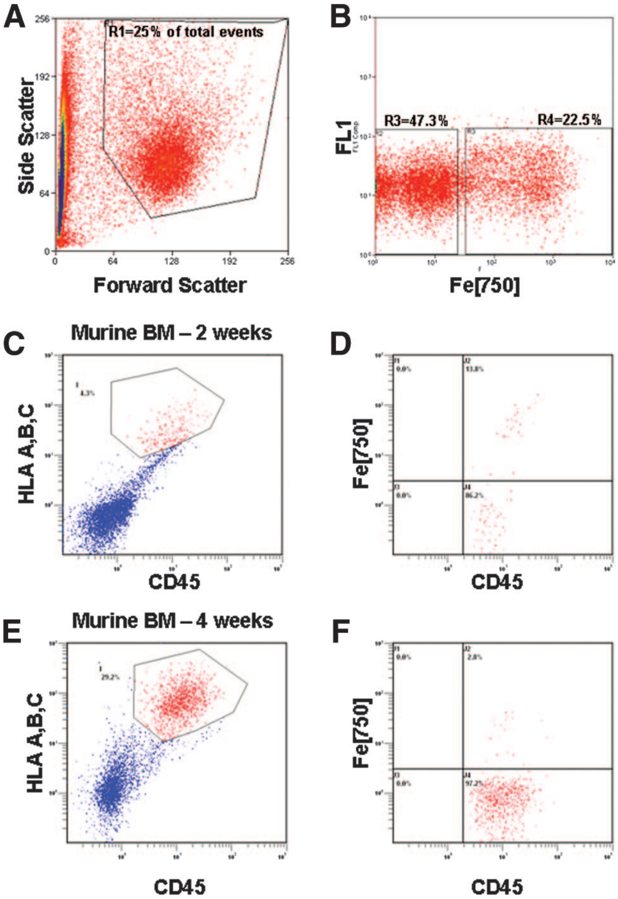

Figure 4. Representative example from the transplantation of Fe[750]-labeled human cells. **(A):** Forward and side scatter plot, with unbound nanoparticles constituting 75% of the counted events. The cells in the R1 gate, 25% of the total events, were fluorescence-activated cell sorting-purified, and the cells were further split into $Fe[750]^{lo}$ (R3 = 47.3%) versus $Fe[750]^{hi}$ (R4 = 22.5%) populations for transplantation **(B)**. Data from the transplantation of the nanoparticle-high cell fraction (R4) are shown below the sorting gates for mice analyzed at 2 weeks **(C, D)** and 4 weeks **(E, F)** after transplantation of the labeled cells. Abbreviations: BM, bone marrow; HLA, human leukocyte antigen.

number of the injected cells had lodged in the spleen, as well as the BM. These data demonstrate that the $Fe[750]^{hi}$ cells can be detected easily in the marrow following i.v. injection of 400,000 labeled cells. The bone images in Figure 5D are from a mouse injected intrafemorally with the same labeled cell population (4×10^5 $Fe[750]^{hi}CD34^+$ cells).

The bone images shown in Figure 5B and 5F demonstrate the importance of eliminating unbound particles from the cell population to be injected. These mice were injected intrafemorally with free particles, and there was a resulting strong signal in each case. The spleen from the mouse injected i.v. with free particles was very bright (Fig. 5F), indicating nonspecific lodgment of the nanoparticles in spleen tissue. Another control is shown in Figure 5E, where PBS alone was injected, and only minimal background autofluorescence was observed in both marrow and spleen. The samples shown in Figure 5 were all imaged on the same day, in direct comparison with one another.

In summary, the images show that mice that had received an i.v. or i.f. injection of FACS-sorted $Fe[750]^{hi}CD34^+$ cells had higher signal in the femur and tibia, as compared with the control mice that had received PBS or $Fe[750]^{lo}CD34^+$ cells. Free particles (as well as nonsorted bulk cultures transplanted into the mice; data not shown) displayed high signals comparable to the signal of FACS-sorted $Fe[750]^+CD34^+$ cells. These data demonstrate that purification of the $Fe[750]^+CD34^+$ population is a necessary step prior to imaging to ensure that the signal observed is due to migrating cells rather than to free nanoparticles lodging in the tissue.

Discussion

Quiescent human HSC are difficult to label using viral vectors or other modalities to allow tracking in vivo. Here, we present a rapid method to label and directly monitor human cell engraftment using flow cytometry in combination with fluorescence imaging. Two commercially available agents, Feridex and protamine sulfate, formed stable complexes capable of efficiently labeling human HSC subsets. Previous studies have demonstrated that Pro-Fe labeling does not adversely affect the viability of human progenitor cells [11]. Our results extend these observations to immunodeficient mice to evaluate the repopulation capacity of nanoparticle-labeled, highly purified human cells. By conjugating fluorophore to the dextran coat of Feridex, signals generated from labeled human HSC subsets could be measured by both flow cytometry and fluorescence imaging. Traditional staining with Prussian blue for counting iron oxide-labeled cells provides little information about labeling efficiencies or cell type. Here, flow cytometry analysis allowed direct assessment of the number of labeled cells with a cell specific marker, such as CD34 in vitro or human-specific CD45 in vivo, to better define the labeled population.

The current model provides an improvement over the other, previously described systems because the fluorescent tag allows flow-based sorting of labeled cells to remove the nonlabeled cells and unbound beads, to obtain a clean population of labeled cells prior to transplantation. We are injecting a pure population into the animals. This is an improvement over other sorting methods, such as magnetic sorting, where "free" unbound particles are also captured for injection. Our data indicate that the unbound particles can confound initial interpretations because they may be sequestered in areas of damage or inflammation. These unbound particles will likely be phagocytosed by murine macrophages, but for early time points it is possible that they can mask or confuse results, so removal is optimal.

Since Feridex is biologically inactive, the primary cellular uptake mechanism of the protamine-sulfate-complexed Feridex particles may occur through endosomal capture, endocytosis [14, 38], or membrane-mediated interaction with the Pro-Fe complex. Loading differences between human HSC from different sources might reflect differences in membrane properties or corresponding cellular activity, such as metabolic quiescence and low ATP levels. However, the current studies demonstrate that highly quiescent human hematopoietic stem/progenitor cells can be labeled with nanoparticles to efficiencies equivalent to those of dividing cells. Other reporter labeling methods, such as viral transduction, require that the cells be actively cycling [33, 34]. Interestingly, adding more Fe[750] to the cultures did not result in higher numbers of labeled $CD34^+$ cells. Furthermore, increasing the protamine sulfate concentration did not affect the loading protocol. The optimal protamine sulfate concentration observed in this study was 1 μg/ml, which is in accordance with other published data [11]. At concentrations greater than 20 μg/ml, an increasing number of $CD34^+$ cells became unhealthy or nonviable (data not shown).

Cohorts of immune-deficient mice received sorted Fe[647]- or Fe[750]-labeled $CD34^+$ cells, for comparison to cells cultured in

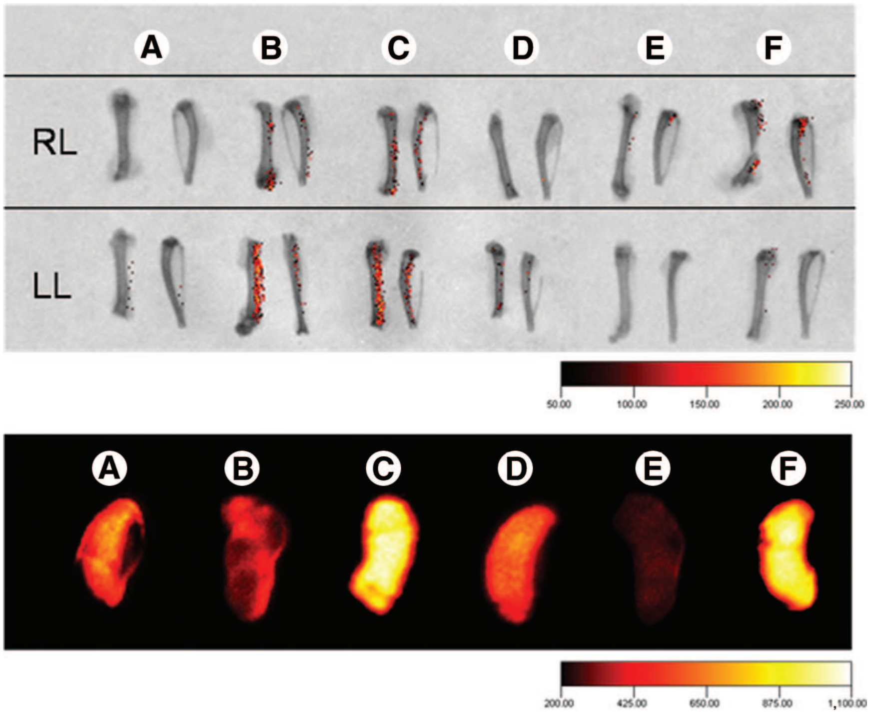

Figure 5. Fluorescence imaging of engrafted cells in the bone marrow and spleen. Representative examples of NOD/SCID β2M-null mice that received transplants of 4×10^5 Fe[750]^{lo}CD34$^+$ cells by i.v. injection **(A)**, free Fe[750] by intrafemoral (i.f.) injection **(B)**, 4×10^5 Fe[750]^{hi}CD34$^+$ cells by i.v. injection **(C)**, 4×10^5 Fe[750]^{hi}CD34$^+$ cells by i.f. injection **(D)**, phosphate-buffered saline **(E)**, and free Fe[750] by i.f. injection **(F)**. The LL was injected in all i.f. mice except for that shown in **(F)**, where the RL was injected with free particles. Abbreviations: LL, left leg; RL, right leg.

the same way, but without nanoparticle labeling. Flow cytometry measurements of flushed femurs and tibia of the recipient animals revealed the presence of labeled CD34$^+$ and human-specific CD45$^+$ cells. At weeks 1 and 2 post-transplantation, labeled CD45$^+$ cells could be observed in the bone marrow of the recipient animals, but the nanoparticle label dropped by weeks 3 and 4. These data indicate that as the cells begin to divide there is a decrease in the detection of nanoparticle-labeled cells. Thus, one disadvantage of nanoparticle-labeling techniques is evident in the data, that is, dilution of the signal by cell division or cell death. It is interesting that the nanoparticle$^+$ and CD45$^+$ levels both increased over the first 2 weeks postinjection, which mirrors previously published data showing continual recruitment to the marrow compartment during this period of time [36]. After injection, stem and progenitor cells lodge in the lung, spleen, and liver and then seed from those organs to the marrow space, because of higher levels of stromal-derived factor (SDF-1) produced there. SDF-1, the ligand for CXCR4 on stem/progenitor cells, is the most potent chemotactic signal for primitive stem cells. Our data recapitulate this continuing accrual to the marrow and will provide other laboratories with a method to further query these homing events. Therefore, it would appear that initially the cells are not expanding within the marrow but are migrating there. Cashman et al. have demonstrated that human cells transplanted into immune-deficient mice do not divide much in the marrow space for the first 2 weeks postinjection, but in week 3, there begins to be an expansion [39], and our data fit with this report.

For the first time, in the current study, Fe[647]- and Fe[750]-labeled CD34$^+$ cells were FACS-sorted prior to transplantation. Purification of Feridex-labeled cells by centrifugation, filtration, or magnetic separation methods results in a contaminated target cell population. Although magnetic sorting results in the removal of unlabeled cells, free, unbound particles still remained in the cell solution. FACS analysis of bulk cultures shows that more than 75%–90% of counted events arise from free Fe[750] in solution, if the cells are not first sorted to remove the unbound particles. Removal of excess nanoparticles by FACS ensured that the population used for transplantation was more than 99% pure and that the in vivo detection was not an artifact arising from unbound particles.

The nanoparticles used in this study inherently contain T2* properties that allow them to be imaged by MRI as described by a number of groups [3, 4, 7, 11, 38]. Attempts to acquire MRI images of the spleen and bone marrow in live animals failed at the cell doses used in our experiment (4×10^5). However, other groups have reported detecting labeled cells in the bone marrow and spleen in animals transplanted with 1×10^7 cells [3], and Anderson et al. detected migrated iron-labeled Sca1$^+$ cells in implanted glioma in mice using only 5×10^5 iron-positive cells [40]. Perhaps slightly increasing our cell transplantation number or using a model such as tumor targeting, which allows a more focused migration in vivo, could result in noninvasive imaging for tracking of human stem cell subsets in vivo by MRI. When transplanting primary hematopoietic stem/progenitor cells, the engraftment is diffuse throughout many tissues.

Using the current techniques, flow cytometry analysis gating on CD34$^+$ or CD45$^+$ expression and Fe[750] confirms the presence of human cells residing in the BM. Using this method, we propose that as few as 1×10^5 Fe[750]$^+$CD34$^+$ cells residing in the bone marrow can be detected by fluorescence imaging. Beyond 2 weeks, the human cell expansion, egress from the marrow, and iron metabolism began to dilute the nanoparticle signal below the limit of detection of both techniques. The current data demonstrate that transient labeling of repopulating HSC subsets with fluorescent nanoparticles is a powerful and novel tool for dynamic tracking of human stem cells during the initial weeks after transplantation.

ACKNOWLEDGMENTS

This work was supported by the NIH, National Institutes of Diabetes and Digestive and Kidney Diseases (Grants 2R01DK61848 and 2R01DK53041 [to J.A.N.]), National Heart, Lung and Blood Institute (Grant R01HL073256 [to J.A.N.]), and National Cancer Institute (P50-CA94056 [to D.P.-W.]).

D.A.H. is supported by the Juvenile Diabetes Research Foundation. D.J.M., J.B., D.A.H., S.A.H., and R.L. performed the research. All authors contributed to experimental design. M.H.C., D.P.-W., and J.A.N. analyzed the data. D.J.M., J.B., D.A.H., D.P.-W., and J.A.N. wrote the paper. D.J.M. and J.B. contributed equally to this work.

Disclosure of Potential Conflicts of Interest

The authors indicate no potential conflicts of interest.

References

1 Bonde J, Hess DA, Nolta JA. Recent advances in hematopoietic stem cell biology. Curr Opin Hematol 2004;11:392–398.
2 Hacein-Bey-Abina S, von Kalle C, Schmidt M et al. A serious adverse event after successful gene therapy for X-linked severe combined immunodeficiency. N. Engl J Med 2003;348:255–256.
3 Daldrup-Link H, Rudelius M, Piontek G et al. Migration of iron oxide-labeled human hematopoietic progenitor cells in a mouse model: In vivo monitoring with 1.5-T MR imaging equipment. Radiology 2005;234:197–205.
4 Daldrup-Link HE, Rummeny EJ, Ihssen B et al. Iron-oxide-enhanced MR imaging of bone marrow in patients with non-Hodgkin's lymphoma: Differentiation between tumor infiltration and hypercellular bone marrow. Eur Radiol 2002;12:1557–1566.
5 Daldrup-Link HE, Rudelius M, Ooostendorp R et al. Comparison of iron oxide labeling properties of hematopoietic progenitor cells from umbilical cord blood and from peripheral blood for subsequent in vivo tracking in a xenotransplant mouse model. Acad Radiol 2005;12:502–510.
6 Kircher M, Allport J, Graves E et al. In vivo high resolution three-dimensional imaging of antigen-specific cytotoxic T-lymphocyte trafficking to tumors. Cancer Res 2003;63:6838–6846.
7 Lewin M, Carlesso N, Tung CH et al. Tat peptide-derivatized magnetic nanoparticles allow in vivo tracking and recovery of progenitor cells. Nat Biotechnol 2000;18:410–414.
8 Weissleder R, Cheng HC, Bogdanova A. Magnetically labeled cells can be detected by MR imaging. J Magn Reson Imaging 1997;7:258–263.
9 Arbab A, Bashaw L, Miller B et al. Characterization of biophysical and metabolic properties of cells labeled with superparamagnetic iron oxide nanoparticles and transfection agent for cellular MR imaging. Radiology 2003;229:838–846.
10 Arbab AS. Intracytoplasmic tagging of cells with ferumoxides and transfection agent for cellular magnetic resonance imaging after cell transplantation: Methods and techniques. Transplantation 2003;76:1123–1130.
11 Arbab AS. Efficient magnetic cell labeling with protamine sulfate complexed to ferumoxides for cellular MRI. Blood 2004;104:1217–1223.
12 Arbab AS. Comparison of transfection agents in forming complexes with ferumoxides, cell labeling efficiency, and cellular viability. Mol Imaging 2004;3:24–32.
13 Frank JA, Miller BR, Arbab AS et al. Clinically applicable labeling of mammalian and stem cells by combining superparamagnetic iron oxides and transfection agents. Radiology 2003;228:480–487.
14 Hogemann D, Josephson L, Weissleder, R., Basilion JP. Improvement of MRI probes to allow efficient detection of gene expression. Bioconjug Chem 2000;11:941–946.
15 Josephson L, Tung CH, Moore A et al. High-efficiency intracellular magnetic labeling with novel superparamagnetic-Tat peptide conjugates. Bioconjug Chem 1999;10:186–191.
16 Koch A, Reynolds F, Kirscher M et al. Uptake and metabolism of a dual fluorochrome Tat-nanoparticle in HeLa cells. Bioconjug Chem 2003;14:1115–1121.
17 Zhao M, Kircher M, Josephson L et al. Differential conjugation of Tat peptide to superparamagnetic nanoparticles and its effect on cellular uptake. Bioconjug Chem 2002;13:840–844.
18 Hess DA, Meyerrose TE, Wirthlin L et al. Functional characterization of highly purified human hematopoietic repopulating cells isolated according to aldehyde dehydrogenase activity. Blood 2004;104:1648–1655.
19 Kida T, Yokota M, Masuyama A et al. A facile synthesis of polyglycidyl ethers from polyols and epichlorohydrin. Synthesis 1993;487–489.
20 Stookey LL. Ferrozine, a new spectrophotometric reagent for iron. Anal Chem 1970;42:779–781.
21 Dao MA, Nolta JA. Cytokine and integrin stimulation synergize to promote higher levels of GATA-2, c-myb, and CD34 protein in primary human hematopoietic progenitors from bone marrow. Blood 2007;109:2373–2379.
22 Hanenberg H, Hashino K, Konishi H et al. Optimization of fibronectin-assisted retroviral gene transfer into human CD34+ hematopoietic cells. Hum Gene Ther 1997;8:2193–2206.
23 Pollok KE, Hanenberg H, Noblitt TW et al. High-efficiency gene transfer into normal and adenosine deaminase-deficient T lymphocytes is mediated by transduction on recombinant fibronectin fragments. J Virol 1998;72:4882–4892.
24 Dao MA, Hashino K, Kato I et al. Adhesion to fibronectin maintains regenerative capacity during ex vivo culture and transduction of human hematopoietic stem and progenitor cells. Blood 1998;92:4612–4621.
25 Christianson SW, Greiner DL, Hesselton RA et al. Enhanced human CD4+ T cell engraftment in beta2-microglobulin-deficient NOD-scid mice. J Immunol 1997;158:3578–3586.
26 Kollet O, Peled A, Byk T et al. beta2 microglobulin-deficient (B2m(null)) NOD/SCID mice are excellent recipients for studying human stem cell function. Blood 2000;95:3102–3105.
27 Dao MA, Taylor N, Nolta JA. Reduction in levels of the cyclin-dependent kinase inhibitor p27(kip-1) coupled with transforming growth factor beta neutralization induces cell-cycle entry and increases retroviral transduction of primitive human hematopoietic cells. Proc Natl Acad Sci U S A 1998;95:13006–13011.
28 Dao MA, Hwa J, Nolta JA. Molecular mechanism of transforming growth factor beta-mediated cell-cycle modulation in primary human CD34(+) progenitors. Blood 2002;99:499–506.
29 Metz S, Bonaterra G, Rudelius M et al. Capacity of human monocytes to phagocytose approved iron oxide MR contrast agents in vitro. Eur Radiol 2004;14:1851–1858.
30 Raynal I, Prigent P, Peyramaure S et al. Macrophage endocytosis of superparamagnetic iron oxide nanoparticles: Mechanisms and comparison of ferumoxides and ferumoxtran-10. Invest Radiol 2004;39:56–63.
31 Rogers WJ, Basu P. Factors regulating macrophage endocytosis of nanoparticles: Implications for targeted magnetic resonance plaque imaging. Atherosclerosis 2005;178:67–73.
32 Sipe JC, Filippi M, Martino G et al. Method for intracellular magnetic labeling of human mononuclear cells using approved iron contrast agents. Magn Reson Imaging 1999;17:1521–1523.
33 Miller DG, Adam MA, Miller AD. Gene transfer by retrovirus vectors occurs only in cells that are actively replicating at the time of infection [published erratum appears in Mol Cell Biol 1992;12:433]. Mol Cell Biol 1990;10:4239–4242.
34 Sutton RE, Reitsma MJ, Uchida N et al. Transduction of human progenitor hematopoietic stem cells by human immunodeficiency virus type 1-based vectors is cell cycle dependent. J Virol 1999;73:3649–3660.
35 Kohn DB, Sadelain M, Dunbar C et al. American Society of Gene Therapy (ASGT) ad hoc subcommittee on retroviral-mediated gene transfer to hematopoietic stem cells. Mol Ther 2003;8:180–187.
36 Oostendorp R, Ghaffari S, Eaves C. Kinetics of in vivo homing and recruitment into cycle of hematopoietic cells are organ-specific but CD44-independent. Bone Marrow Transplant 2000;26:559–566.
37 Arbab AS, Wilson LB, Ashari P et al. A model of lysosomal metabolism of dextran coated superparamagnetic iron oxide (SPIO) nanoparticles: Implications for cellular magnetic resonance imaging. NMR Biomed 2005;18:383–389.
38 Daldrup-Link HEea. Targeting of hematopoietic progenitor cells with MR contrast agents. Radiology 2003;228:760–767.
39 Cashman J, Lapidot T, Wang J et al. Kinetic evidence of the regeneration of multilineage hematopoiesis from primitive cells in normal human bone marrow transplanted into immunodeficient mice. Blood 1997;89:4307–4316.
40 Anderson SA, Glod J, Arbab AS et al. Noninvasive MR imaging of magnetically labeled stem cells to directly identify neovasculature in a glioma model. Blood 2005;105:420–425.